PNAS
www.pnas.org

Supplementary Information for

Emergence of homochirality in large molecular systems

Gabin Laurent, David Lacoste and Pierre Gaspard

Corresponding author : Gabin Laurent
E-mail: gabin.laurent@espci.fr

This PDF file includes:

Supporting Information Text

S1. The multiplication of chiral molecules with their number of atoms

The number of species that are chiral are observed to increase faster with their number of atoms, than the number of achiral species, in spite of the fact that diatomic and triatomic molecules are achiral and only tetratomic molecules can be chiral (in their ground electronic state). In particular, studies of alkane and monosubstituted alkane stereoisomers (1) show that the numbers of chiral C_k and achiral A_k species are growing exponentially with their number k of carbon atoms according to

$$C_k \sim \Lambda^k \qquad \text{and} \qquad A_k \sim \Lambda^{k/2} \qquad \text{with} \qquad \Lambda \simeq 3.287112 \tag{S1}$$

for $k \gg 1$. As a consequence, chiral molecules become overwhelmingly dominant for a large enough number of atoms.

Now, the question is to determine when the crossover occurs between a world of small molecules dominated by achiral species and a world dominated by chiral molecules, which is likely to become homochiral by spontaneous symmetry breaking induced in the non-equilibrium reaction network.

In order to answer this question, we have investigated the fractions of achiral and chiral species as functions of the number of atoms in each molecule. Such fractions can be defined by counting the pairs of enantiomers either once or twice. The numbers of achiral and chiral species with n heavy atoms being respectively denoted A_n and C_n, on the one hand, the fractions defined by counting once the pairs of enantiomers are given by

$$f_n^{(\mathrm{A})} \equiv \frac{A_n}{A_n + C_n} \qquad \text{and} \qquad f_n^{(\mathrm{C})} \equiv \frac{C_n}{A_n + C_n}, \tag{S2}$$

such that $f_n^{(\mathrm{A})} + f_n^{(\mathrm{C})} = 1$, in which case, the crossover happens for n_1 atoms in the molecule such that

$$A_{n_1} = C_{n_1} \, . \tag{S3}$$

On the other hand, the fractions defined by counting twice the pairs of enantiomers are given by

$$\tilde{f}_n^{(\mathrm{A})} \equiv \frac{A_n}{A_n + 2C_n} \qquad \text{and} \qquad \tilde{f}_n^{(\mathrm{C})} \equiv \frac{2C_n}{A_n + 2C_n}, \tag{S4}$$

such that $\tilde{f}_n^{(\mathrm{A})} + \tilde{f}_n^{(\mathrm{C})} = 1$ in which other case, the crossover happens for n_2 atoms in the molecule such that

$$A_{n_2} = 2C_{n_2} \, . \tag{S5}$$

Since C_n becomes larger than A_n as n increases, we should expect that $n_2 < n_1$.

A. Monosubstituted alkane stereoisomers. Achiral and chiral monosubstituted alkanes $\mathrm{C}_k\mathrm{H}_{2k+1}\mathrm{X}$ have been enumerated in Ref. (1). In particular, Table 1 of Ref. (1) gives the numbers of achiral A_k and chiral C_k monosubstituted alkanes as stereoisomers versus the number k of carbon atoms they contain and this up to $k = 100$. Using these data, the fractions of achiral and chiral stereoisomers have been obtained and they are shown in Fig. S1 by counting once or twice the enantiomeric pairs.

We observe that the crossover occurs at $k_1 \simeq 5.7$ or $k_2 \simeq 4.7$, depending on whether the pairs of enantiomers are counted once or twice. As expected, we have that $k_2 < k_1$. Now, the result is that the crossover happens for a relatively small number of carbon atoms. Here, the carbon atoms and the substituted atom X determine the geometry of the molecule. Here, the temperature is supposed to be high enough such that hydrogen atoms rotate and vibrate fast enough that the chirality is determined by the skeleton of the carbon and X atoms.

B. Alkane stereoisomers. The stereoisomers of alkanes $\mathrm{C}_k\mathrm{H}_{2k+2}$ have also been studied and the enumeration of achiral and chiral alkanes is given in Ref. (2). Table 3 of Ref. (2) gives the numbers of achiral A_k and chiral C_k alkanes as stereoisomers versus the number k of carbon atoms they contain and this up to $k = 100$. The fractions of achiral and chiral stereosiomers obtained with these data are plotted in Fig. S2.

Here, we see that the crossover occurs at $k_1 \simeq 9.5$ if the pairs of enantiomers are counted once and at $k_2 \simeq 8.4$ if they are counted twice. Again, the crossover happens for a relatively small number of carbon atoms (which are the atoms determining the molecular geometry). The crossover happens for somewhat larger molecules because alkanes have molecular structures that are more symmetric than in the presence of one substitution, thus delaying the crossover as the number of determining atoms increases.

C. Chemical Universe. In Ref. (3), all the possible molecules up to 11 atoms of C, N, O, and F were generated by considering simple valency, chemical stability, and synthetic feasibility rules, and they were collected in a database containing 26.4 million molecules and 110.9 million stereoisomers. Fig. 5 of Ref. (3) shows the fractions of achiral and chiral molecules in the database as a function of their size characterized by the number of heavy atoms. Here, the crossover happens for $n_1 \simeq 8.5 \pm 0.1$. This virtual exploration of the chemical universe clearly demonstrates the prevalence of chirality for large enough molecules.

D. Analysis of the PubChem database.

D.1. Raw data. The raw database of PubChem contains 139 millions of species. In the following, we will restrict our analysis to species which contain less than 20 heavy atoms (*i.e.*, atoms heavier than hydrogen). There are two reasons for this choice, on one hand the statistics becomes more limited for molecules much longer than 20, and on the other hand, there is a discontinuity in the number of achiral and chiral molecules in the PubChem database as shown in Fig. S3a. We have contacted the curators of the database, but there is no information currently available about the origin of this discontinuity. In any case, we should avoid this problem by staying below 20.

From the complete dataset downloaded from PubChem, 91,606,016 molecules were analyzed after rejection of compounds with isotopic elements, multiple components or incomplete data on bond structure. From the 33,563,343 molecules with less than 21 heavy atoms, 18,705,878 molecules (55.7 %) are chiral, and 1,376,672 chiral molecules have no stereocenters (7.4 % of the chiral molecules with less than 21 heavy atoms) thus for these molecules their chirality depends only on their non planar geometry.

As shown in Fig. S3b, the analysis of the 33,563,343 molecules with less than 21 heavy atoms of the database in terms of their fraction of chiral and non-chiral species shows a crossover around $n_{\rm raw} \simeq 9.4$. A crossover in this region is coherent with an increase in the number of stereoisomers per molecule for molecules of this length.

D.2. Methods of generation of stereoisomers and enantiomers. Chiral species in the PubChem database were detected using the chiral flag present in the list of SDF files which contains information about the structure of the molecules in the database.

For the generation of enantiomers, a list of non-canonical SMILES formulas was built, which contains information about defined stereocenters. For each chiral molecule with an available SMILES formula (*e.g.*, C[**C@@**](CC1CC=C(C(=C1)O)O)(C(=O)O)N), one generates a mirror image of it (*i.e.*, C[**C@**](CC1CC=C(C(=C1)O)O)(C(=O)O)N for the latter example), and then one searches it in the list. If it is not found, then it is added to the list in the expanded database. However, for chiral centers that do not explicitly appears in the SMILES formula, one cannot find them and reverse them with a simple method and this creates an uncertainty in the final number of chiral molecules due to missed generated enantiomers. Thus a fraction of enantiomers cannot be generated due to incomplete data in the PubChem database.

For the generation of stereoisomers, one looks whether the database contains the theoretical maximum number of stereoisomers for a given species, which can be evaluated from the number of defined stereocenters. If all the stereoisomers are not present, which is frequent for molecules containing several stereocenters, the database is expanded so that each chiral species has the maximum possible number of stereoisomers (*i.e.*, 2^{n^*} with n^* the number of stereocenters in the molecule). However, this procedure does not count properly the meso forms, which should be labeled as achiral although they contain stereocenters due to an internal symmetry.

Now, after generating enantiomers as explained previously, one obtains Fig. S4.

Then, stereoisomers were generated using the procedure described previously, giving Fig. 1a of the main article where 47,452,700 steoisomers have been added to complete the PubChem dataset. In this case, the intersection occurs at $n_2 \simeq 6.4$ for if both enantiomers are considered and $n_1 \simeq 8.1$ if only one enantiomer is considered.

D.3. Error bars. In this subsection, we explain how error bars were obtained in the graph of achiral and chiral fractions. For molecules with i atoms, the number of chiral molecules is denoted $\mathcal{N}_i$ and the one of achiral molecules $\mathcal{M}_i$. These numbers are taken as independent Poisson distributions with a parameter given by their mean number, *i.e.*, by $\mathcal{N}_i$ and $\mathcal{M}_i$ themselves. The fraction of chiral molecules is given by

$$x_i = \frac{\mathcal{N}_i}{\mathcal{M}_i + \mathcal{N}_i} \,. \qquad [S6]$$

The error on x_i thus reads

$$\sigma_{x_i} = x_i(1-x_i)\left(\frac{1}{\sqrt{\mathcal{M}_i}} + \frac{1}{\sqrt{\mathcal{N}_i}}\right). \qquad [S7]$$

The model does not capture systematic errors, but only the statistical errors in the counting of $\mathcal{N}_i$ or $\mathcal{M}_i$.

S2. Separating the mean from fluctuations in the Jacobian matrix

We now study the properties of the $N \times N$ Jacobian matrix $\mathbf{J}$ with $N = N_{\rm C}$ introduced in the Materials and Methods of the main text. For large complex networks, this matrix may be supposed to be random because of fluctuations in the values of its elements for the different reactions and species. Let us separate the mean of the elements of $\mathbf{J}$ from their fluctuations in the following way:

$$\mathbf{J} = \mu\,\mathbf{1} + \sigma\,\mathbf{G} \qquad [S8]$$

where $\mathbf{1}$ is the matrix full of elements equal to 1 and $\mathbf{G}$ has elements distributed according to independent Gaussian distributions of zero mean and unit variance:

$$\langle G_{ab}\rangle = 0\,, \qquad \langle G_{ab}G_{cd}\rangle = \delta_{ac}\delta_{bd}\,. \qquad [S9]$$

Accordingly, the mean value of Eq. [S8] gives

$$\langle \mathbf{J}\rangle = \mu\,\mathbf{1}\,, \qquad [S10]$$

allowing us to determine the parameter μ as the mean value of the elements of the matrix $\mathbf{J}$:

$$\mu = \frac{1}{N^2}\sum_{a,b=1}^{N} J_{ab}\,. \qquad [S11]$$

Moreover, the parameter σ can be evaluated by the root mean square of the matrix elements,

$$\sigma = \frac{1}{N}\left[\sum_{a,b=1}^{N}(J_{ab}-\mu)^2\right]^{1/2}, \qquad [S12]$$

as a consequence of Eq. [S9].

The matrix full of ones has the eigenvalues $\{N,0,0,...,0\}$ and it can be diagonalized with an orthogonal transformation $\mathbf{O}$ composed of the eigenvectors $\mathbf{v}=\{\cos[2\pi k(m-1)/N]\}_{k=1}^{N}$ with $m=1,2,...,N$ (after their normalization). The eigenvector corresponding to the eigenvalue equal to N is thus given by $m=1$ in the expression of the latter eigenvectors. Accordingly,

$$\begin{aligned}\mathbf{J}'=\mathbf{O}^{\mathrm{T}}\cdot\mathbf{J}\cdot\mathbf{O} &= \mu\,\mathbf{O}^{\mathrm{T}}\cdot\mathbf{1}\cdot\mathbf{O}+\sigma\,\mathbf{O}^{\mathrm{T}}\cdot\mathbf{G}\cdot\mathbf{O}\\ &= \mu\begin{pmatrix} N & 0 & 0 & \dots & 0\\ 0 & 0 & 0 & \dots & 0\\ 0 & 0 & 0 & \dots & 0\\ \vdots & \vdots & \vdots & \ddots & \vdots\\ 0 & 0 & 0 & \dots & 0\end{pmatrix}+\sigma\,\mathbf{G}'\end{aligned} \qquad [S13]$$

with the matrix

$$\mathbf{G}'=\mathbf{O}^{\mathrm{T}}\cdot\mathbf{G}\cdot\mathbf{O}\,. \qquad [S14]$$

This latter is again a random matrix with elements

$$G'_{ij}=\sum_{a,b}(\mathbf{O}^{\mathrm{T}})_{ia}G_{ab}(\mathbf{O})_{bj} \qquad [S15]$$

distributed according to independent Gaussian distribution of zero mean and unit variance. Indeed, we have that

$$\langle G'_{ij}\rangle=\sum_{a,b}(\mathbf{O}^{\mathrm{T}})_{ia}\langle G_{ab}\rangle(\mathbf{O})_{bj}=0 \qquad [S16]$$

and

$$\begin{aligned}\langle G'_{ij}G'_{kl}\rangle &= \sum_{a,b,c,d}(\mathbf{O}^{\mathrm{T}})_{ia}(\mathbf{O})_{bj}(\mathbf{O}^{\mathrm{T}})_{kc}(\mathbf{O})_{dl}\langle G_{ab}G_{cd}\rangle\\ &= \sum_{a}(\mathbf{O}^{\mathrm{T}})_{ia}(\mathbf{O})_{ak}\sum_{b}(\mathbf{O}^{\mathrm{T}})_{jb}(\mathbf{O})_{bl}=\delta_{ik}\,\delta_{jl}\,.\end{aligned} \qquad [S17]$$

If $\mu\neq 0$ and $\sigma\neq 0$, the eigenvalue problem can thus be solved by perturbation theory in the small parameter $\zeta=\sigma/(\mu N)$. Therefore, in the limit $N\to\infty$, the spectrum of the matrix $\mathbf{J}$ is composed of the eigenvalue

$$\lambda^{(1)}=\mu\,N+O(N^0) \qquad [S18]$$

and $N-1$ eigenvalues $\{\lambda^{(m)}\}_{m=2}^{N}$ contained inside the disk of radius $\sigma\sqrt{N}$ in the complex plane $(\Re\,\lambda,\Im\,\lambda)$ with probability one in the limit $N\to\infty$. The probability density of these latter eigenvalues is similar as for the real Ginibre ensemble in the limit $N\to\infty$ (4). In the general case where the matrix elements have non-Gaussian distributions and/or are statistically correlated, the dominant eigenvalue behaves as described by Eq. [S18], but the $N-1$ non-dominant eigenvalues may have different kinds of probability distribution.

S3. General instability criterion

Now using the results of section S2 for random matrices with Gaussian independent and identically distributed elements, we conclude that when $\mu N\geq\sigma\sqrt{N}$, which is equivalent to $N\geq(\sigma/\mu)^2$, an isolated eigenvalue will be dominant as in mechanism (i). If this condition is satisfied, the instability occurs when $\mu N\geq 1/\tau$, in other words when the number of chiral species $N=N_{\mathrm{C}}$ is such that $N_{\mathrm{C}}\geq\max\{1/(\tau\mu),(\sigma/\mu)^2\}$ with $\mu>0$.

Instead when $N\leq(\sigma/\mu)^2$, the previous eigenvalue is no longer dominant and the instability can only occur due to eigenvalues that are located at the edge of the Girko circle (5), which is the second mechanism (ii). This edge, which corresponds to eigenvalues with a maximum real part, can be made of either a single real eigenvalue or to a pair of conjugated complex valued eigenvalues. The instability then occurs when $N\geq 1/(\tau\sigma)^2$, or taken together when $(\sigma/\mu)^2\geq N\geq 1/(\tau\sigma)^2$.

We note that the first mechanism (i) holds with $\mu>0$ even for a vanishing root mean square $\sigma=0$, but the second mechanism (ii) requires that the root mean square σ is not equal to zero.

According to this analysis, a non-equilibrium reaction network with sufficiently many chiral species is likely to undergo spontaneous chiral symmetry breaking. We now discuss a specific implementation for a chemical reaction network.

S4. Generalized Frank's model

The basic idea is that there exist more chiral than achiral species. Frank's model (6) is thus generalized by multiplying the species, especially, the chiral species. Moreover, the reverse reactions are included in order to possibly satisfy microreversibility. The reaction network is given by Eqs. [3]-[4]-[5] of the main text with $\mathrm{E}_i = \mathrm{D}_i$ and $\bar{\mathrm{E}}_i = \mathrm{L}_i$, reading

$$\mathrm{A}_a + \mathrm{D}_i \rightleftharpoons \mathrm{D}_j + \mathrm{D}_k \,, \tag{S19}$$

$$\mathrm{A}_a + \mathrm{L}_i \rightleftharpoons \mathrm{L}_j + \mathrm{L}_k \,, \tag{S20}$$

$$\mathrm{D}_i + \mathrm{L}_j \rightleftharpoons \tilde{\mathrm{A}}_b + \tilde{\mathrm{A}}_c \,, \tag{S21}$$

with $a = 1, 2, \ldots, N_\mathrm{A}$; $b, c = 1, 2, \ldots, \tilde{N}_{\tilde{\mathrm{A}}}$; and $i, j, k = 1, 2, \ldots, N_\mathrm{C}$. The net reaction rates are given by

$$w^{(\mathrm{D})}_{aijk} = k_{+aijk} A_a D_i - k_{-aijk} D_j D_k \qquad \text{with} \qquad j \le k \,, \tag{S22}$$

$$w^{(\mathrm{L})}_{aijk} = k_{+aijk} A_a L_i - k_{-aijk} L_j L_k \qquad \text{with} \qquad j \le k \,, \tag{S23}$$

$$\tilde{w}_{bcij} = \tilde{k}_{-bcij} D_i L_j - \tilde{k}_{+bcij} \tilde{A}_b \tilde{A}_c \qquad \text{with} \qquad b \le c \,, \tag{S24}$$

where the positive sign in the subscripts of the rate constants refers to the direction of chirality generation. We note that $\tilde{k}_{\pm bcij} = \tilde{k}_{\pm bcji}$ because of the mirror symmetry [15]. The kinetic equations are thus given by

$$\dot{A}_d = -\sum_{\substack{aijk \\ j \le k}} \delta_{da}\, w^{(\mathrm{D})}_{aijk} - \sum_{\substack{aijk \\ j \le k}} \delta_{da}\, w^{(\mathrm{L})}_{aijk} + \frac{1}{\tau}(A_{0d} - A_d) \,, \tag{S25}$$

$$\dot{D}_m = \sum_{\substack{aijk \\ j \le k}} \nu_{m,ijk}\, w^{(\mathrm{D})}_{aijk} - \sum_{\substack{bcij \\ b \le c}} \delta_{mi}\, \tilde{w}_{bcij} + \frac{1}{\tau}(D_{m0} - D_m) \,, \tag{S26}$$

$$\dot{L}_m = \sum_{\substack{aijk \\ j \le k}} \nu_{m,ijk}\, w^{(\mathrm{L})}_{aijk} - \sum_{\substack{bcij \\ b \le c}} \delta_{mj}\, \tilde{w}_{bcij} + \frac{1}{\tau}(L_{m0} - L_m) \,, \tag{S27}$$

$$\dot{\tilde{A}}_e = \sum_{\substack{bcij \\ b \le c}} (\delta_{eb} + \delta_{ec})\, \tilde{w}_{bcij} + \frac{1}{\tau}(\tilde{A}_{0e} - \tilde{A}_e) \,, \tag{S28}$$

where

$$\nu_{m,ijk} \equiv -\delta_{mi} + \delta_{mj} + \delta_{mk} \,. \tag{S29}$$

The rate constants can be taken according to log-normal distributions (7). If the rate constants are distributed around some mean values with relatively small root mean squares, the leading behavior can be determined by replacing the rate constants with their mean value. In this respect, we may assume that all the rate constants are equal,

$$\tilde{k}_{\pm abij} = \tilde{k}_\pm \,, \qquad k_{\pm aijk} = k_\pm \qquad (\forall\ a, b, i, j, k) \,, \tag{S30}$$

and the concentrations of achiral species, D-, and L-enantiomers can also be supposed to be equal

$$A_a = A \,, \qquad D_i = D \,, \qquad L_i = L \,, \qquad \text{and} \qquad \tilde{A}_a = \tilde{A} \,, \qquad (\forall\ a, i) \,. \tag{S31}$$

Thus, the kinetic equations become

$$\dot{A} = -\frac{N_\mathrm{C}}{N_\mathrm{A}} \left[(K_+ A\, D - K_- D^2) + (K_+ A\, L - K_- L^2) \right] + \frac{1}{\tau}(A_0 - A) \,, \tag{S32}$$

$$\dot{D} = (K_+ A\, D - K_- D^2) - (\tilde{K}_- D L - \tilde{K}_+ \tilde{A}^2) + \frac{1}{\tau}(D_0 - D) \,, \tag{S33}$$

$$\dot{L} = (K_+ A\, L - K_- L^2) - (\tilde{K}_- D L - \tilde{K}_+ \tilde{A}^2) + \frac{1}{\tau}(L_0 - L) \,, \tag{S34}$$

$$\dot{\tilde{A}} = 2\, \frac{N_\mathrm{C}}{\tilde{N}_{\tilde{\mathrm{A}}}} (\tilde{K}_- D L - \tilde{K}_+ \tilde{A}^2) + \frac{1}{\tau}(\tilde{A}_0 - \tilde{A}) \,, \tag{S35}$$

with the effective rate constants:

$$K_\pm \equiv \frac{N_\mathrm{A} N_\mathrm{C} (N_\mathrm{C} + 1)}{2}\, k_\pm \qquad \text{and} \qquad \tilde{K}_\pm \equiv \frac{\tilde{N}_{\tilde{\mathrm{A}}} (\tilde{N}_{\tilde{\mathrm{A}}} + 1) N_\mathrm{C}}{2}\, \tilde{k}_\pm \,. \tag{S36}$$

As a consequence of these kinetic equations, we have that

$$N_\mathrm{A}\, \dot{A} + N_\mathrm{C}\, \dot{D} + N_\mathrm{C}\, \dot{L} + \tilde{N}_{\tilde{\mathrm{A}}} \dot{\tilde{A}} = \frac{1}{\tau}\big[(N_\mathrm{A}\, A_0 + N_\mathrm{C}\, D_0 + N_\mathrm{C}\, L_0 + \tilde{N}_{\tilde{\mathrm{A}}}\, \tilde{A}_0) - (N_\mathrm{A}\, A + N_\mathrm{C}\, D + N_\mathrm{C}\, L + \tilde{N}_{\tilde{\mathrm{A}}}\, \tilde{A}) \big] \,, \tag{S37}$$

implying

$$\lim_{t\to\infty}(N_{\rm A}\,A+N_{\rm C}\,D+N_{\rm C}\,L+\tilde{N}_{\tilde{\rm A}}\,\tilde{A})=N_{\rm A}\,A_0+N_{\rm C}\,D_0+N_{\rm C}\,L_0+\tilde{N}_{\tilde{\rm A}}\,\tilde{A}_0\,. \qquad [S38]$$

The model is compatible with the existence of equilibrium. Indeed, the detailed balance conditions give the following Guldberg-Waage equilibrium relations,

$$\frac{D_{\rm eq}}{A_{\rm eq}}=\frac{L_{\rm eq}}{A_{\rm eq}}=\frac{K_+}{K_-} \qquad \text{and} \qquad \frac{\tilde{A}_{\rm eq}}{A_{\rm eq}}=\frac{K_+}{K_-}\sqrt{\frac{\tilde{K}_-}{\tilde{K}_+}}\,. \qquad [S39]$$

Therefore, equilibrium exists for any positive value of the rate constants and two rate constants can independently take arbitrarily small values.

In the fully irreversible regime with $K_-=0$ and $\tilde{K}_+=0$, we further suppose that the system is only supplied with the achiral species of high free energy: $D_0=L_0=\tilde{A}_0=0$. Since Eq. [S38] holds for long enough time, we have that

$$A=A_0-\frac{N_{\rm C}}{N_{\rm A}}\,(D+L)-\frac{\tilde{N}_{\tilde{\rm A}}}{N_{\rm A}}\,\tilde{A}\,. \qquad [S40]$$

Therefore, the kinetic equations reduce to the three following equations:

$$\dot{D} = K_+D\left[A_0-\frac{N_{\rm C}}{N_{\rm A}}\,(D+L)-\frac{\tilde{N}_{\tilde{\rm A}}}{N_{\rm A}}\,\tilde{A}\right]-\tilde{K}_-DL-\frac{1}{\tau}\,D\,, \qquad [S41]$$

$$\dot{L} = K_+L\left[A_0-\frac{N_{\rm C}}{N_{\rm A}}\,(D+L)-\frac{\tilde{N}_{\tilde{\rm A}}}{N_{\rm A}}\,\tilde{A}\right]-\tilde{K}_-DL-\frac{1}{\tau}\,L\,, \qquad [S42]$$

$$\dot{\tilde{A}} = 2\,\frac{N_{\rm C}}{\tilde{N}_{\tilde{\rm A}}}\,\tilde{K}_-DL-\frac{1}{\tau}\,\tilde{A}\,. \qquad [S43]$$

Setting

$$\Delta\equiv K_+A_0-\frac{1}{\tau}=\frac{N_{\rm C}(N_{\rm C}+1)}{2}\,k_+\,N_{\rm A}\,A_0-\frac{1}{\tau}\,, \qquad [S44]$$

the steady states and their eigenvalues $\{\xi_1,\xi_2,\xi_3\}$ of linear stability are here given by

$$D=L=\tilde{A}=0: \qquad \xi_1=\xi_2=\Delta\,,\ \xi_3=-1/\tau\,, \qquad [S45]$$

$$D=0\,,\ L=\frac{N_{\rm A}\,\Delta}{N_{\rm C}\,K_+}\,,\ \tilde{A}=0: \qquad \xi_1=-\frac{N_{\rm A}\,\tilde{K}_-\,\Delta}{N_{\rm C}\,K_+}\,,\ \xi_2=-\Delta\,,\ \xi_3=-1/\tau\,, \qquad [S46]$$

$$D=\frac{N_{\rm A}\,\Delta}{N_{\rm C}\,K_+}\,,\ L=0\,,\ \tilde{A}=0: \qquad \xi_1=-\Delta\,,\ \xi_2=-\frac{N_{\rm A}\,\tilde{K}_-\,\Delta}{N_{\rm C}\,K_+}\,,\ \xi_3=-1/\tau\,, \qquad [S47]$$

$$D=L=\frac{N_{\rm A}\,\Delta}{2N_{\rm C}\,K_++N_{\rm A}\,\tilde{K}_-}+O(\Delta^2)\,,\ \tilde{A}=O(\Delta^2): \qquad \xi_1=\frac{N_{\rm A}\,\tilde{K}_-\,\Delta}{2N_{\rm C}\,K_++N_{\rm A}\,\tilde{K}_-}+O(\Delta^2)\,,\ \xi_2=-\Delta+O(\Delta^2)\,,\ \xi_3=-1/\tau+O(\Delta^2)\,. \qquad [S48]$$

In these expressions, the terms $O(\Delta^2)$ are negligible if

$$\frac{N_{\rm A}\,N_{\rm C}\,K_+\,\tilde{K}_-\,\tau\,\Delta}{(2N_{\rm C}\,K_++N_{\rm A}\,\tilde{K}_-)^2}\ll 1\,. \qquad [S49]$$

The behavior is determined by the parameter [S44]. Since concentrations are always non-negative, the only steady state that exists if $\Delta<0$ is the trivial racemic state [S45], which is an attractor because $\xi_1,\xi_2,\xi_3<0$ in this case. If $\Delta>0$, three new steady states emerge, which are the L-homochiral attractor [S46], the D-homochiral attractor [S47], and the non-trivial racemic state [S48]. This latter is unstable since $\xi_1>0$ for this new steady state. The threshold of instability towards homochirality is thus found at $\Delta=0$. Therefore, spontaneous chiral symmetry breaking happens if the following criterion is satisfied,

$$k_+\,\tau\,N_{\rm A}\,A_0>\frac{2}{N_{\rm C}(N_{\rm C}+1)}\,, \qquad [S50]$$

which is Eq. [6] of the main text in the case $\langle k_+\rangle=k_+$ where all the rate constants are equal.

Now, if the rate constants were not all equal as in Eq. [S30], but if they were statistically distributed, the analysis carried out here above would provide the mean behavior of the system. However, the statistical distribution of the rate constants would introduce further effects that should also be analyzed. In particular, for every steady state, the matrix of linear stability could be decomposed in a similar way as in Eq. [S8] into a mean value that would be given by Eq. [S11] and fluctuations of root mean square [S12]. The leading eigenvalue of this random matrix could thus be evaluated as in section S2, giving an estimation comparable to the eigenvalues ξ_i obtained here above and this for every stable or unstable steady state.

Similar results hold for the other models with either $\mathrm{E}_m=\mathrm{D}_m$ and $\bar{\mathrm{E}}_m=\mathrm{L}_m$ or $\mathrm{E}_m=\mathrm{L}_m$ and $\bar{\mathrm{E}}_m=\mathrm{D}_m$ for each enantiomeric pairs $m=1,2,\ldots,N_{\rm C}$.

S5. Instability criterion of the trivial racemic state for the generalized Frank model

Spontaneous chiral symmetry breaking can be investigated by considering the linear stability analysis of any racemic solution with the stationary concentrations $\mathbf{D} = \mathbf{L}$ where $\mathbf{D} = \{D_i\}_{i=1}^N$ and $\mathbf{L} = \{L_i\}_{i=1}^N$. For this purpose, we introduce the variables

$$\delta\mathbf{X} \equiv \frac{1}{2}\left(\delta\mathbf{L} - \delta\mathbf{D}\right), \tag{S51}$$

characterizing infinitesimal deviations with respect to the racemic subspace. These deviations are ruled by the following set of linear equations:

$$\frac{d}{dt}\delta\mathbf{X} = \mathsf{M}\cdot\delta\mathbf{X}, \tag{S52}$$

with the matrix

$$\mathsf{M} = \mathsf{J} - \frac{1}{\tau}\,\mathsf{I} = \frac{\partial\dot{\mathbf{D}}}{\partial\mathbf{D}} - \frac{\partial\dot{\mathbf{D}}}{\partial\mathbf{L}}, \tag{S53}$$

since the fundamental chiral symmetry of the kinetic equations implies that

$$\frac{\partial\dot{\mathbf{D}}}{\partial\mathbf{D}} = \frac{\partial\dot{\mathbf{L}}}{\partial\mathbf{L}} \qquad \text{and} \qquad \frac{\partial\dot{\mathbf{D}}}{\partial\mathbf{L}} = \frac{\partial\dot{\mathbf{L}}}{\partial\mathbf{D}}\,. \tag{S54}$$

For the irreversible model we consider, we have the matrix elements

$$\begin{aligned} M_{mn} &= J_{mn} - \frac{1}{\tau}\,\delta_{mn} = \frac{\partial\dot{D}_m}{\partial D_n} - \frac{\partial\dot{D}_m}{\partial L_n} = \sum_{\substack{i\\ m\le i}} k_{+nmi}\,A + \sum_{\substack{i\\ i\le m}} k_{+nim}\,A \\ &+ \tilde{k}_{-mn}\,D_m - \delta_{mn}\left(\sum_{\substack{ij\\ i\le j}} k_{+nij}\,A + \sum_i \tilde{k}_{-mi}\,L_i + \frac{1}{\tau}\right), \end{aligned} \tag{S55}$$

where A and $D_i = L_i$ are the concentrations of the stationary racemic solution. Since the rate constants are supposed to be statistically distributed, this is also the case for the stationary concentrations $\{D_i\}_{i=1}^N$ and $\{L_i\}_{i=1}^N$ and thus for the matrix elements J_{mn}. The statistical distribution of the matrix elements J_{mn} depends on the reaction network and may be complicated, but they could be decomposed as explained in section S2 into a mean value given by Eq. [S11] and fluctuations of root mean square [S12].

At the trivial racemic fixed point such that $D_i = L_i = \tilde{A} = 0$ for all species i and $A = A_0$, the elements [S55] of the Jacobian matrix associated with the evolution of the enantiomeric excess are evaluated by

$$M_{mn} = J_{mn} - \frac{1}{\tau}\,\delta_{mn} = A_0\left(\sum_{\substack{i\\ m\le i}} k_{+nmi} + \sum_{\substack{i\\ i\le m}} k_{+nim}\right) - \delta_{mn}\left(A_0\sum_{\substack{ij\\ i\le j}} k_{+nij} + \frac{1}{\tau}\right). \tag{S56}$$

Thus the matrix M can be decomposed into three matrices Q and R as

$$\mathsf{M} = \mathsf{J} - \frac{1}{\tau}\,\mathsf{I} = A_0\,\mathsf{Q} - A_0\,\mathsf{R} - \mathsf{I}/\tau\,. \tag{S57}$$

where I is the identity, the elements of matrix Q are given by

$$Q_{mn} = \sum_{\substack{i\\ m\le i}} k_{+nmi} + \sum_{\substack{i\\ i\le m}} k_{+nim}\,, \tag{S58}$$

which are sums of $N_C + 1$ random variables of mean $\langle k_+\rangle$ and standard deviation σ_{k_+} (the element k_{+nmm} occurs twice, once in each sum). Finally, R is a diagonal matrix of elements

$$R_{nn} = \sum_{\substack{ij\\ i\le j}} k_{+nij}\,. \tag{S59}$$

According to the central limit theorem, in the large N_C limit, the elements of Q are distributed following a Gaussian distribution of mean $\mu_Q = \langle k_+\rangle(N_C+1)$ and standard deviation $\sigma_Q = \sigma_{k_+}\sqrt{N_C+1}$. Moreover, the elements of the matrix R are also randomly distributed according to a Gaussian of mean $\mu_R = \langle k_+\rangle N_C(N_C+1)/2$ and standard deviation $\sigma_R = \sigma_{k_+}\sqrt{N_C(N_C+1)/2}$. Unfortunately, although the spectra of the matrices Q and R are known, it is not possible to deduce immediately from these the spectrum of M, because these matrices are not diagonal in the same base.

One can however still use perturbation theory. For the matrix Q, we use the same decomposition in terms of a full matrix of ones plus a correction G:

$$\mathsf{Q} = \mu_Q\,\mathbf{1} + \sigma_Q\,\mathsf{G}\,, \tag{S60}$$

and we decompose the matrix $\mathbf{R}$ as

$$\mathbf{R} = \mu_R\,\mathbf{I} + \mathbf{H}\,, \tag{S61}$$

where $\mathbf{H}$ is a diagonal matrix with subdominant terms as compared to μ_R (this follows from the law of large numbers). In the end, this means we can decompose $\mathbf{M}$ as

$$\mathbf{M} = \mathbf{P} + A_0\,\sigma_Q\,\mathbf{G} - A_0\,\mathbf{H}\,. \tag{S62}$$

where $\mathbf{P} = A_0\mu_Q\mathbf{1} - \left(A_0\mu_R + \tau^{-1}\right)\mathbf{I}$. The largest eigenvalue of $\mathbf{P}$ is $A_0(N_C\mu_Q - \mu_R) - \tau^{-1} = A_0\langle k_+\rangle N_C(N_C+1)/2 - \tau^{-1}$, and this eigenvalue can be shown to be dominant using the same perturbation calculation as done before.

For the system to be unstable, this dominant eigenvalue must be positive. Thus, the threshold above which the system is unstable is

$$\langle k_+\rangle\,\tau\,A_0 > \frac{2}{N_C(N_C+1)}\,, \tag{S63}$$

which is Eq. [S50] with the number of achiral species equal to $N_A = 1$. Moreover, Eq. [S50] is recovered when all the rate constants are equal. We note that a deviation from the prediction [S63] is observed when σ_{k_+} becomes large compare to $\langle k_+\rangle$, as depicted in Fig. S5.

One observes that the other eigenvalues of $\mathbf{M}$ do not stay within a Girko circle as shown in Fig. S6. There is no contradiction since the random matrix $\mathbf{M}$ does not have the same statistics for its diagonal and off-diagonal elements, therefore the assumptions of the Girko theorem do not hold anymore (5).

We note that the permutation $\mathrm{D}_m \leftrightarrow \mathrm{L}_m$ for some enantiomeric pair m implies that the corresponding enantiomeric excess changes sign, $\delta X_m \to -\delta X_m$. However, the eigenvalues of the matrix $\mathbf{M}$ remain unchanged under such transformations. This can be shown by the following calculation. Let us denote the eigenvector $\mathbf{u}$ (with eigenvalue p) of the original matrix $\mathbf{M}$, and the new eigenvector $\mathbf{u'}$ (with eigenvalue p') of the transformed matrix $\mathbf{M'}$, obtained after such a permutation, so that

$$\sum_j \mathsf{M}_{ij}\,u_j = p\,u_i \qquad \text{and} \qquad \sum_j \mathsf{M}'_{ij}\,u'_j = p'u'_i\,, \tag{S64}$$

Now, the permutation of the enantiomers means that $\delta X'_i = (-1)^{s_i}\delta X_i$ with $s_i = 1$ if the i^{th} enantiomers are permuted and $s_i = 0$ otherwise. Using Eq. [S52] for the matrices $\mathbf{M}$ and $\mathbf{M'}$, we obtain $M'_{ij} = (-1)^{s_i+s_j}M_{ij}$. It follows from this that the eigenvectors transform as $u'_j = (-1)^{s_j}u_j$ with no change in the eigenvalues $p' = p$. Accordingly, all our results hold for the 2^{N_C-1} models considered.

S6. Two diffusively coupled compartments

We consider here two diffusively coupled compartments containing the same chemical network considered before in a well-mixed situation. In addition, we assume the irreversible regime with $N_A = \tilde{N}_{\tilde{A}} = 1$ and $N_C \gg 1$. The reactions within each compartment read:

$$\mathrm{A}_a + \mathrm{D}_i \to \mathrm{D}_j + \mathrm{D}_k\,, \tag{S65}$$
$$\mathrm{A}_a + \mathrm{L}_i \to \mathrm{L}_j + \mathrm{L}_k\,, \tag{S66}$$
$$\mathrm{D}_i + \mathrm{L}_j \to 2\tilde{\mathrm{A}}_b\,, \tag{S67}$$

where $a, b = 1$ and $i, j, k = 1, \ldots, N_C$ for species in the first compartment, and $a, b = 2$ and $i, j, k = (N_C+1), \ldots, (2N_C)$ for species in the second compartment. In addition, there are transfer reactions between compartments for all the species present:

$$\mathrm{D}_i \rightleftharpoons \mathrm{D}_{i+N_C}, \tag{S68}$$
$$\mathrm{L}_i \rightleftharpoons \mathrm{L}_{i+N_C}, \tag{S69}$$
$$\mathrm{A}_a \rightleftharpoons \mathrm{A}_{a+1}, \tag{S70}$$
$$\tilde{\mathrm{A}}_b \rightleftharpoons \tilde{\mathrm{A}}_{b+1}, \tag{S71}$$

which we assume are characterized by the same transition probability κ (where the convention that $\mathrm{E}_i = \mathrm{E}_{i+2N_C}$ for the concentrations of enantiomers, $\mathrm{A}_a = A_{a+2}$, and $\tilde{\mathrm{A}}_b = \tilde{A}_{b+2}$ is adopted). In the end, the kinetic rate equations of the first reactor are:

$$\dot{A}_d = -\sum_{\substack{aijk\\ j\le k}} \delta_{da}\,w^{(\mathrm{D})}_{aijk} - \sum_{\substack{aijk\\ j\le k}} \delta_{da}\,w^{(\mathrm{L})}_{aijk} + \frac{1}{\tau}(A_{0d} - A_d) + \kappa(A_{d+1} - A_d)\,, \tag{S72}$$

$$\dot{D}_m = \sum_{\substack{aijk\\ j\le k}} \nu_{m,ijk}\,w^{(\mathrm{D})}_{aijk} - \sum_{\substack{bcij\\ b\le c}} \delta_{mi}\,\tilde{w}_{bcij} + \frac{1}{\tau}(D_{m0} - D_m) + \kappa(D_{m+N} - D_m)\,, \tag{S73}$$

$$\dot{L}_m = \sum_{\substack{aijk\\ j\le k}} \nu_{m,ijk}\,w^{(\mathrm{L})}_{aijk} - \sum_{\substack{bcij\\ b\le c}} \delta_{mj}\,\tilde{w}_{bcij} + \frac{1}{\tau}(L_{m0} - L_m) + \kappa(L_{m+N} - L_m)\,, \tag{S74}$$

$$\dot{\tilde{A}}_e = \sum_{\substack{bcij\\ b\le c}} (\delta_{eb} + \delta_{ec})\,\tilde{w}_{bcij} + \frac{1}{\tau}(\tilde{A}_{0e} - \tilde{A}_e) + \kappa(\tilde{A}_{e+1} - \tilde{A}_e), \tag{S75}$$

where $d, e = 1$; $m = 1, \ldots, N_{\rm C}$; and κ is the diffusive coupling parameter. Similar equations hold for the other reactor, where $d, e = 2$ and $m = (N_{\rm C}+1), \ldots, (2N_{\rm C})$. From these equations one can proceed by using the enantiomeric excess [S51] which obeys as before the equation:

$$\frac{d}{dt}\delta\mathbf{X} = \mathbf{M}\cdot\delta\mathbf{X}\,, \tag{S76}$$

with the matrix

$$\mathbf{M} \equiv \frac{\partial\dot{\mathbf{D}}}{\partial\mathbf{D}} - \frac{\partial\dot{\mathbf{D}}}{\partial\mathbf{L}}\,. \tag{S77}$$

Now the matrix $\mathbf{M}$ has the following block structure

$$\mathbf{M} = \begin{pmatrix} \mathbf{M}_1 - \kappa\mathbf{I} & \kappa\mathbf{I} \\ \kappa\mathbf{I} & \mathbf{M}_2 - \kappa\mathbf{I} \end{pmatrix},$$

where $\mathbf{M}_{1,2}$ represent the Jacobian matrix of compartments $1, 2$ respectively and $\mathbf{I}$ is the identity matrix of same dimension. In the limit of small κ, we can treat the effect of diffusion as a small perturbation. This perturbation will introduce a correction of the order of κ on the eigenvalues of the uncoupled case ($\kappa = 0$). Since the dominant eigenvalues in the uncoupled case are of the order of $\sqrt{N_{\rm C}}$ or $N_{\rm C}$, depending on whether the scenario (i) or (ii) is relevant, this correction should have a small effect on the threshold of instability.

Let us call $\mathbf{u}_1$ (resp. $\mathbf{u}_2$) the eigenvectors of the matrix $\mathbf{M}_1$ (resp. $\mathbf{M}_2$) and the corresponding eigenvalues p_1 and p_2. A simple calculation provides the eigenvectors $\mathbf{u}$ and the eigenvalues p of the matrix $\mathbf{M}$ as function of $\mathbf{u}_{1,2}$ and $p_{1,2}$. In the case where the dominant eigenvalues of $\mathbf{M}_{1,2}$ are $p_1 = p_2 = \mu N_{\rm C} \pm O(\sigma)$ for both submatrices, one finds that the dominant contribution to p equals either $\mu N_{\rm C}$ or $\mu N_{\rm C} - 2\kappa$. The corresponding dominant eigenvectors have respectively uniform components across both compartments: $\mathbf{u} = (1, \ldots, 1)^{\rm T}$ or opposite components on each compartment: $\mathbf{v} = (1, \ldots, 1, -1, \ldots, -1)^{\rm T}$. The synchronization towards a global homochiral state occurs when the contribution of $\mathbf{u}$ wins over that of $\mathbf{v}$ on long times. Therefore, one then finds that such a synchronization should occur approximately when $\kappa \simeq \sigma/2$.

Another way to look at the synchronization of the states of the two compartments is to consider the evolution of the averaged enantiomeric excess in both compartments, defined by

$$\delta\bar{X}_i = \frac{1}{2}\left(\delta X_i + \delta X_{i+N_{\rm C}}\right). \tag{S78}$$

The equation of evolution of that quantity is controlled by a matrix $\bar{M}_{mn}$ such that

$$\bar{M}_{mn} = \frac{1}{2}\left(M_{mn} + M_{m+N_{\rm C},n}\right). \tag{S79}$$

In the notation of section S5, this may be written as

$$\bar{M}_{mn} = A_0 Q_{mn} - \frac{1}{2}\delta_{mn}(A_0 R_{mm} + 1/\tau) - \frac{1}{2}\delta_{m+N_{\rm C},n}(A_0 R_{mm} + 1/\tau), \tag{S80}$$

where we have used that $Q_{mn} = Q_{m+N_{\rm C},n}$ and $R_{m+N_{\rm C},m+N_{\rm C}} = R_{mm}$. This property holds since the rate constants take exactly the same values in both compartments because the chemical composition and reactions in the two compartments are exactly the same. Although the concentrations of species take different values in the two compartments, their values do not enter in the stability of the trivial racemic fixed point. It follows from Eq. [S80], that the eigenvalues of the matrix $\bar{M}$ are exactly the ones we had before in the well-mixed case. From our study of the well-mixed case, we expect that the average enantiomeric excess should undergo an instability when the driving is sufficiently large. If the average enantiomeric excess reaches extremal values 1 or -1 at long times, then the two compartments must be both homochiral of the same chirality.

Using numerical simulations, we have confirmed this scenario. Firstly, when diffusion is weak for $\kappa \to 0$, we recover the previous scenario for a transition to homochirality, separately holding in each compartment As κ increases, so does the coupling between the two compartments. If there is a small bias present which is the same in the two compartments (L for instance), then one ends up with a homochiral state which is L in that case. The interesting case is therefore when the two compartments are given an opposite small bias initially. Then, as shown in Fig. S7, we find that as κ increases, we go from a global racemic state at small values of κ towards a global homochiral state when the coupling is sufficiently strong. The threshold of instability is found not to be significantly changed as compared to the well-mixed case in agreement with the theoretical argument given above. In addition, the threshold where the transition occurs is indeed of the order of $\sigma = 2 \times 10^{-4}$.

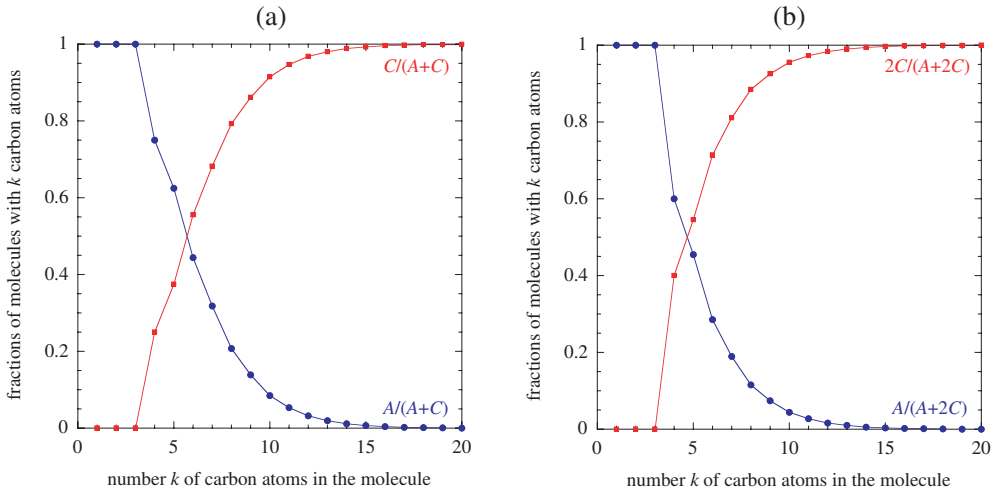

Fig. S1. Fractions of achiral and chiral stereoisomers of monosubstituted alkanes versus the number k of carbon atoms in the molecule, counting (a) once and (b) twice the pairs of enantiomers. The data are from Ref. (1).

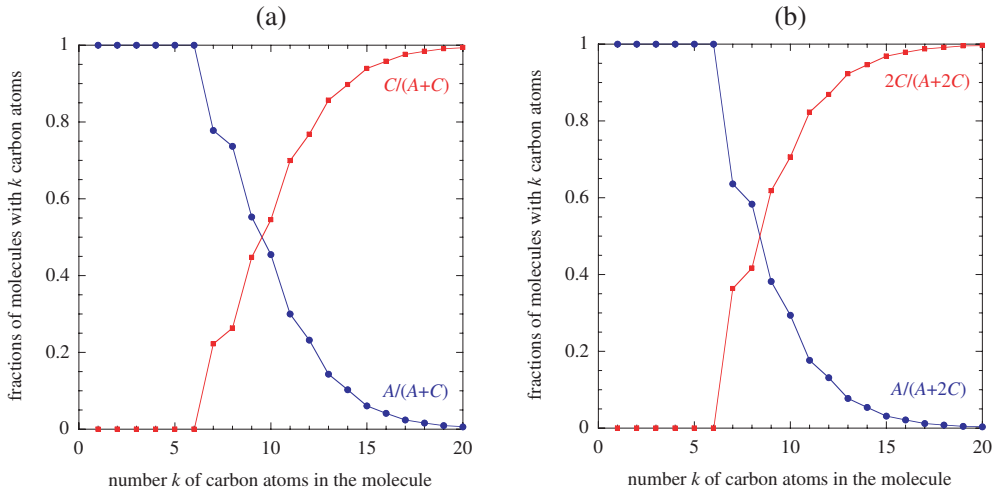

Fig. S2. Fractions of achiral and chiral stereoisomers of alkanes versus the number k of carbon atoms in the molecule, counting (a) once and (b) twice the pairs of enantiomers. The data are from Ref. (2).

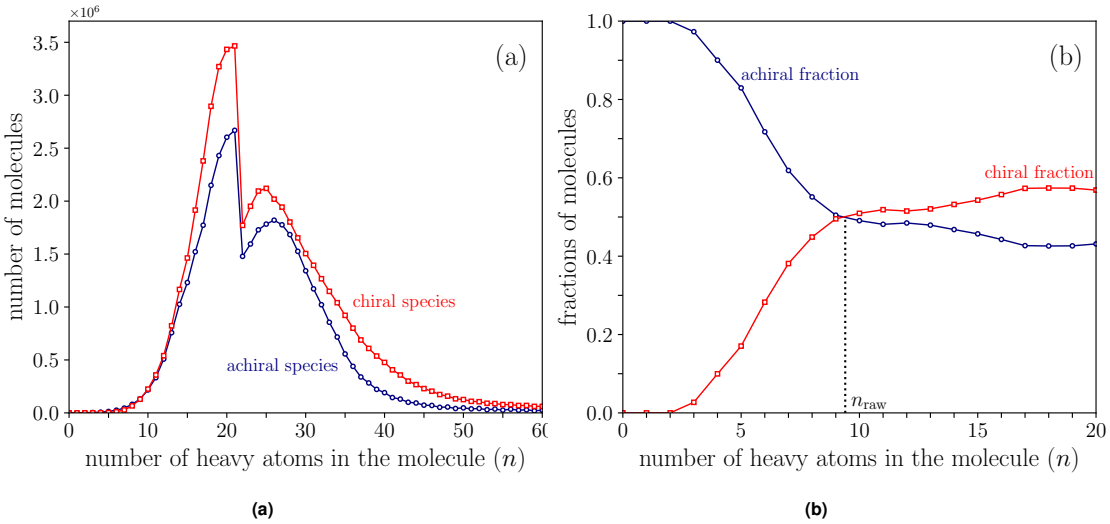

(a) **(b)**

Fig. S3. (a) Total number of achiral and chiral species in the raw PubChem database containing about 139 millions of species. (b) Fractions of chiral and achiral molecules containing $n \leq 20$ heavy atoms. In this case, only $N = 33,563,343$ molecules with $n \leq 20$ heavy atoms were analyzed after the specific selection. The figure on the right shows an intersection at $n_{\rm raw} \simeq 9.4$.

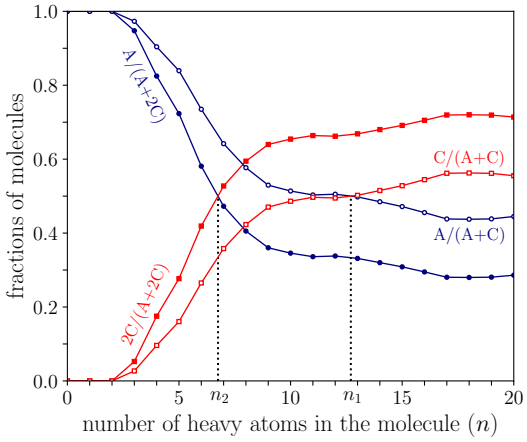

Fig. S4. Analysis of the database expanded in enantiomers, with $N = 50,252,957$ molecules in data ($i.e.$, $16,689,614$ enantiomers were generated) with $n \leq 20$ heavy atoms. The intersection occurs at $n_2 \simeq 6.7$ for if both enantiomers are considered and $n_1 \simeq 12.7$ if only one enantiomer is considered.

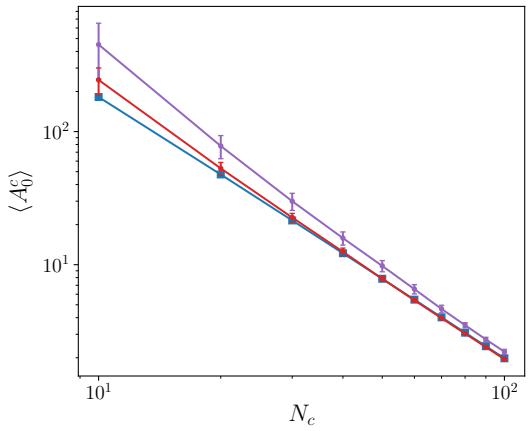

Fig. S5. Comparison between the observed control parameter value A_0 at the transition with the theoretical prediction given by Eq. [6] of the main text (blue solid line) after averaging over 100 realizations of the rate constants for different standard deviation σ_{k_+} and $\sigma_{\tilde{k}_-}$ of rate constants : $\sigma_{k_+} = \sigma_{\tilde{k}_-} = 10^{-3}$ (red), $\sigma_{k_+} = \sigma_{\tilde{k}_-} = 10^{-2}$ (purple), while $\langle k_+ \rangle = \langle \tilde{k}_- \rangle = 10^{-4}$.

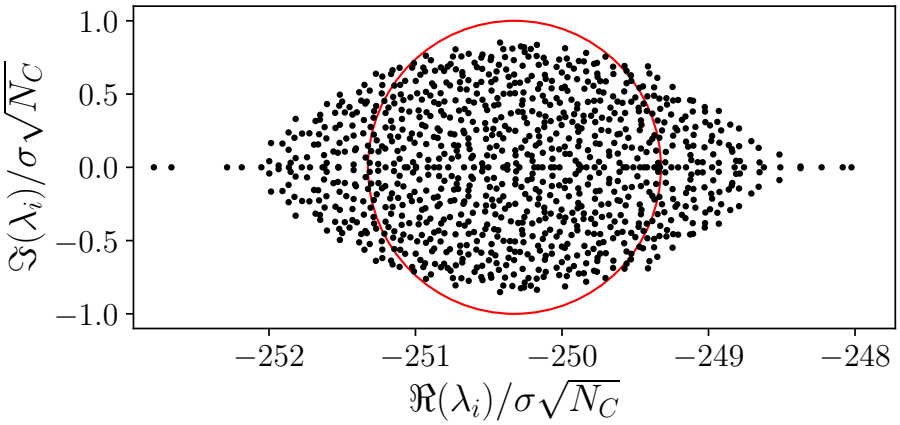

Fig. S6. Close-up of the non-dominant eigenvalues of the Jacobian matrix **M** of the generalized Frank model, which do no fill the Ginibre circle. Here, the matrix **M** characterizes a system of $N_C = 1000$ chiral species, with rate constants distributed according to a log-normal distribution of parameters $\langle k_+ \rangle = 10^{-4}$ and $\sigma_{k_+} = 2 \times 10^{-4}$ and $\tau = 1$. The parameter $A_0 = 25$, is far beyond the instability threshold for the trivial racemic state. The dominant eigenvalue is around 250 and lies outside the field of view for these parameters. The red circle is the unit circle, and the normalization factor $1/\sigma\sqrt{N_C}$ is expressed in term of $\sigma = A_0\sigma_Q$ with $\sigma_Q = \sigma_{k_+}\sqrt{N_C + 1}$, which is the standard deviation of the matrix **Q** elements in the decomposition of the matrix **M** in section S5.

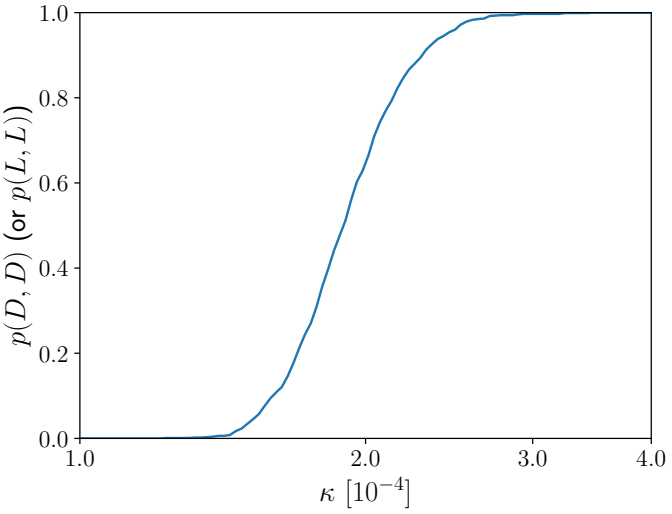

Fig. S7. Probability to have two homochiral compartments of the same chirality on long times (either both are D or both are L) as function of the transition probability of transfer of molecules between the two compartments κ. The initial condition is such that there is an opposite chiral bias in both compartments, so that in the absence of diffusion coupling, the global state will be racemic. For one realization of the rate constants, the parameter κ is varied; then this procedure is repeated for different realizations of the rate constants. The curve has been done for a value of the driving force which is above the instability threshold. Simulations were carried out with an initial enantiomeric excess $\epsilon_1 = 10^{-2}$ and D- and L-enantiomers concentrations of all chiral species were initialized at $D_0 = 2 + \epsilon_1$ and $L_0 = 2 - \epsilon_1$ in the first compartment and with $\epsilon_2 = 1.5 \times 10^{-2}$ in the second compartment but favoring L-enantiomers. The unactivated achiral specie was initialized at $\tilde{A}_0 = 0$ and the activated one at $A_0 = 80$, far above the homochirality threshold in each compartment. All the constants k_{+ijk} and $\tilde{k}_{-ij}$ follow a log-normal distribution of parameters $\mu = -10.02$ and $\sigma = 1.27$ (*i.e.*, corresponding to a log-normal distribution with $\langle k_+ \rangle = \langle \tilde{k}_- \rangle = 10^{-4}$ and $\sigma_{k_+} = \sigma_{\tilde{k}_-} = 2 \times 10^{-4}$), with $\tilde{k}_{ij} = \tilde{k}_{ji}$ to satisfy the mirror symmetry described in Eq. (S16). The number of chiral species was set up to $N_C = 20$.

References

1. Fujita S (2007) Numbers of monosubstituted alkanes as stereoisomers. *J. Comput. Chem. Jpn.* 6:59–72.
2. Fujita S (2007) Alkanes as stereoisomers. enumeration by the combination of two dichotomies for three-dimensional trees. *MATCH Commun. Math. Comput. Chem.* 57:299.
3. Fink T, Reymond JL (2007) Virtual exploration of the chemical universe up to 11 atoms of C, N, O, F. *J. Chem. Inf. Model* 47:342–353.
4. Ginibre J (1965) Statistical ensembles of complex, quaternion, and real matrices. *J. Math. Phys.* 6(3):440–449.
5. Girko VL (1985) Circular law. *Theory Probab. Appl.* 29(4):694–706.
6. Frank FC (1953) On spontaneous asymmetric synthesis. *Biochim. Biophys. Acta* 11:459–463.
7. Davidi D, Longo LM, Jabłońska J, Milo R, Tawfik DS (2018) A bird's-eye view of enzyme evolution: Chemical, physicochemical, and physiological considerations. *Chem. Rev.* 118(18):8786–8797.